Fernando Bignami, Anna Agliari

A Cournot duopoly model with complementary goods: multistability and complex structures in the basins of attraction.

In this paper we study a Cournot duopoly, proposed by Matsumoto and Nonaka, in which the competitors produce complementary goods and have naive expectations on the production of the opponent. The quantity adjustment mechanism over time evolution is described by a two-dimensional noninvertible map which exhibits complex dynamics and the coexistence of different attractors (multistability). The global behavior of the map is investigated and, in particular, we explain the shape of the basins of attraction of the coexisting attractors and the qualitative changes in their structure, as the transition from a connected basin into a disconnected one. Such a study is motivated by the observation that in dynamical models characterized by multistability the long run outcome is path-dependent and the choice of the initial condition play a crucial role in determining the asymptotic behavior of the system**.**

Keywords:
Cournot duopoly
Noninvertible dynamical model
Multistability
Global bifurcations

A Cournot duopoly model with complementary goods: multistability and complex structures in the basins of attraction

Fernando Bignami e Anna Agliari
Dipartimento di Scienze Economiche e Sociali
Università Cattolica del Sacro Cuore. Sede di Piacenza
e-mail: fernando.bignami@unicatt.it; anna.agliari@unicatt.it

Gennaio 2006

Contents

1 Introduction

Multistability, i.e., coexistence of several attractors, is an important issue in dynamical economic models and arises quite often when the time evolution is given by the iteration of a nonlinear map. Such situations of coexistence of attractors have been reported for a wide range of nonlinear economic models in discrete time (see, among others, [10], [16], [8], [9], [13], [23], [3]).

In dynamical models characterized by multistability the long run outcome is path-dependent and the choice of the initial condition play a crucial role in determining the asymptotic behavior of the system. Then, when several attractors coexist in the phase-space, the structure of their *basins of attraction*, and the understanding of its dependence on the parameters of the model becomes an important tool in order to have an in-depth knowledge of the environment described by the model. Moreover, a question which arises quite naturally in the case of dynamical systems with multiple attractors is about the nature of the phase-space transitions which lead to the appearance of new attractors or to the disappearance of the existing ones and about the resulting qualitative changes of the structure of the basins.

To get more insights into these questions one is quite naturally led to perform a global analysis of the dynamical system, since the qualitative changes (including appearance/disappearance) of the attractors, and, mainly, the structural changes of the basins of attraction of the coexisting attractors may be due to *global*[1] bifurcations.

The present paper enters in such a framework, analyzing a particular Cournot duopoly, proposed by Matsumoto and Nonaka in [18]. In the economy here considered, two firms are assumed to make production decisions in a strategic context: Indeed the decision making process depends on the mutual choices of the two economic agents. Moreover, they interact repeatedly over time and, due to a lack of information, they adopt a trial-and-error method, so that the production choices evolve over time following a nonlinear dynamical model. The reaction functions, i.e. the functions showing how the supply of each firm depends on that of the competitor, are quadratic functions and this fact, after the works of Rand, [24], and Poston & Stewart, [21], is known to possibly lead to complex dynamics.

Several studies on duopoly models having reaction functions of such a type have been recently proposed in literature, among others we recall [22], [5], [6], [8]. The main difference between the model here studied and those analyzed in the cited papers, regards the shape of the reaction functions: The producer of this model are faced with U-shaped reaction functions, while they have an upside down parabola shape in the other papers. The basic economic assumption leading to U-shaped reaction function is that goods are considered complementary, and not perfect substitute, as usually it occurs in duopoly theory. Indeed, the complementarity of the productions implies that the price of a good increases with the quantity of the other one (that is a positive sale externality),

[1] I.e. bifurcations that are not associated with the behavior of the linearization of the dynamical system around its steady states or cycles.

so that the decisions of each firm are positively affected by the production of the competitor.

While in the paper of Matsumoto and Nonaka [18] the emphasis was on chaotic dynamics, the present paper focalizes on the global dynamic behavior of the trajectories of the model. Our goal is the analysis of the multistability situations arising in the model; in particular, we are interested in the structures of basins of attractions of the coexisting attractors and in the bifurcations (local and global) causing the appearance/disappearance of attractors and important qualitative changes in the shape of the basins of attraction.

Being the duopoly model described by a discrete time noninvertible dynamical model (i.e. its time evolution is obtained by the iteration of a many-to-one map), the investigation of global bifurcations that change the qualitative structure of the basins is particularly challenging. Indeed in this case the basins may be a multiply-connected or a disconnected set, often made up by the union of infinitely many disjoint portions. In our study we shall make use of the global analysis techniques introduced in the basic books [14], [20] and [1] of some recent results on basin bifurcations in noninvertible maps appeared in [4], [8] and [2].

The paper is organized as follows. In the Section 2, we introduce the model, the time evolution of which is fitted by the iteration of a two-dimensional map T. The main properties of T are studied in Section 3. In particular T is a noninvertible map such that the first component of T^2 depends only on x and the second one only on y (*square separate property*). A feature of the maps having the square separate property is the multistability, i.e. generally they exhibit several coexisting attractors, that may be stable periodic cycles or cyclical chaotic attractors. The analysis of such situation is the aim of Section 4, where the global asymptotic behavior of T is discussed. In particular we identify the set of bounded trajectories (*feasible set*) and, in such a set, we describe the basins of attraction of the different attractors. Generally the feasible set is a connected set, but we shall conclude the section pointing out that in some cases it may also have a complex structure, because the noninvertibility of the map T. Section 5 concludes.

2 The model

The model we are interested in has been recently proposed by Matsumoto and Nonaka, [18], and describes the strategic choices of two firms producing two complementary goods.

The economy is given by two monopolistic firms respectively producing the quantity x_1 in the first market and the quantity x_2 in the second market. The goods sold in the two markets are complementary. We assume that

i) in each market, the inverted demand function is given by

$$p_i\left(x_i, x_j\right) = \alpha_i^2 - \beta_i x_i + \left(\gamma_i x_j\right)^2 \tag{1}$$

where α_i, β_i, γ_i $(i = 1, 2)$ are nonnegative parameters.

ii) the cost functions of the firms are given by

$$C_i(x_i, x_j) = c_i x_i x_j \tag{2}$$

where c_i $(i = 1, 2)$ are nonnegative parameters.

Obviously, the inverse demand functions negatively depend on the quantity of its own product and this dependence is assumed to be linear in (1). The complementary relationship between the two outputs is fitted by the quadratic term in (1), whose effect is to introduce in the model a *positive sale externality*, due to the fact that the sales of one firm are positively influenced by the production of the other firm.

On the supply side, it is assumed, as in [15], that a *negative production externality* exists, the production choices of one firm being influenced by the production level of the other firm in terms of the cost function. Following [18], we confine the analysis to the simple case in which the production cost linearly depends on the other firm's output, and not only on its own.

It is worth to observe that we are considering a situation involving a double externality: A positive one via the market demand, measured by the quadratic term in x_j in (1) and a negative production one via the cost function, due to the dependence on x_j of the marginal cost in (2).

As a consequence, we obtain that the profit of one firm depends on its own output and on that of the competitor as well:

$$\Pi_i = \left(\alpha_i^2 - \beta_i x_i + (\gamma_i x_j)^2\right) x_i - c_i x_i x_j \tag{3}$$

where $i, j = 1, 2$ and $i \neq j$.

Then, each firm acts in a strategic framework, since, when it is choosing the production level, it has to take into account the decisions of the opponent. In particular, the optimal production choice of each firm is given by

$$x_i = r_i(x_j) = \arg\max_{x_i} \Pi_i(x_i, x_j) \qquad i, j = 1, 2 \text{ and } i \neq j \tag{4}$$

The functions $r_1(x_2)$ and $r_2(x_1)$ are called *reaction functions* or *Cournot-Nash reaction functions,* see [12], and are given by

$$r_i(x_j) = \frac{\alpha_i^2 - c_i x_j + (\gamma_i x_j)^2}{2\beta_i} \tag{5}$$

The reaction functions are nonlinear with a parabola shape and crucially depend on the mutual amplitude of the sale and production externalities: Indeed, if $c_i \ll \gamma_i$, the curve is quadratically upward sloping, due to the dominance of the sale externality; whereas, if $\gamma_i \ll c_i$, the reaction function becomes linearly downward sloping, due to the dominance of the production externality.

If the two firms are rational (in the sense that they have full information on the two markets and on the cost profile of the competitor), they choose

immediately one of the intersection points (if any) of the two reaction functions, that is, the so-called *Cournot equilibrium points*. Here we assume the "partial rationality" of the firms and this implies that in making their decision, the producers have to forecast the quantity supplied in the complementary market, i.e.,

$$x_i = r_i\left(x_j^{(e)}\right) = \frac{\alpha_i^2 - c_i x_j^{(e)} + \left(\gamma_i x_j^{(e)}\right)^2}{2\beta_i} \tag{6}$$

where $x_j^{(e)}$ is the expected value of x_j.

Moreover we assume that the decision process is repeated in time and at each stage the firm optimally decides by means of its reaction function (6), assuming that the expected production in the complementary market is the same as in the previous one (as Cournot in his pioneeristic work on duopoly model, [11]):

$$x_j^{(e)}(t) = x_j(t-1) \qquad \forall t > 0. \tag{7}$$

Then the evolution process of the quantities in the two markets is described by the two-dimensional dynamical system

$$M : \begin{cases} x_1(t+1) = \dfrac{\alpha_1^2 - c_1 x_2(t) + (\gamma_1 x_2(t))^2}{2\beta_1} \\ x_2(t+1) = \dfrac{\alpha_2^2 - c_2 x_2(t) + (\gamma_2 x_1(t))^2}{2\beta_2} \end{cases} \tag{8}$$

obtained substituting the expectation mechanism (7) into the reaction function (6) and considering both the markets.

The map M in (8) is nonlinear and depends on 8 parameters $\{\alpha_i, \beta_i, \gamma_i, c_i : i = 1, 2\}$. In order to make simpler the analysis of the dynamical behavior of the trajectories generated by the iteration of M, we follow [18], in which a particular case of the model (8) is considered, given by the two parameter map

$$T : \begin{cases} x' = (\alpha y - \alpha + 1)^2 \\ y' = (\beta x - 1)^2 \end{cases}. \tag{9}$$

In (9), for the sake of simplicity, we denote by x and y the two quantities and the symbol " $'$ " represents the one-period advancement operator, i.e. if x is the production level at time t, then x' denotes the production level at time $t+1$. Comparing the general model (8) with the simpler one (9), it is trivial to obtain the relationships between the parameters, given by

$$\begin{aligned} \gamma_1^2 &= 2\alpha\beta_1,\ c_1^2 = 4\alpha(\alpha-1)\beta_1,\ \alpha_1^2 = 2(\alpha-1)^2\beta_1 \\ \gamma_2^2 &= 2\beta_2\beta^2,\ c_2 = 4\beta\beta_2,\ \alpha_2^2 = 2\beta_2. \end{aligned}$$

Recalling the positivity of the parameters $\{\alpha_i, \beta_i, \gamma_i, c_i : i = 1, 2\}$, we have to study the map T in the parameter space

$$\Omega = \{(\alpha, \beta) : \alpha > 1, \beta > 0\}. \tag{10}$$

In this way, we extend the analysis of Matsumoto and Nonaka, which restricted the study at the parameter set

$$\Omega^{'} = \{(\alpha, \beta) : 1 \leq \alpha \leq 2,\, 0 < \beta \leq 2\}\,.$$

When the parameter constellation belongs to the set $\Omega^{'}$, the map T is a transformation of the set $[0,1] \times [0,1]$ into itself and any divergent trajectory is avoided.

Instead, in the set Ω divergent trajectories (and then unfeasible from an economic point of view) are a possible outcome, but for any value of (α, β) we shall identify suitable *strategic sets* $\boldsymbol{F}_1$ and $\boldsymbol{F}_2$ for the two firms, i.e., sets from which the production choices x and y are taken. They have to be such that, given an initial condition $(x_0, y_0) \in \boldsymbol{F}_1 \times \boldsymbol{F}_2$, a trajectory (also called *Cournot tâtonnement*) $\{x_t, y_t\} = T^t\,(x_0, y_0)$, $t \geq 0$, where T^t is the t^{th} iterate of map T, remains bounded. The set $S = \boldsymbol{F}_1 \times \boldsymbol{F}_2$ is called set of *feasible points* (or *feasible trajectories*).

3 Properties of the map T

In this Section we study some properties of the Cournot tâtonnement given by iteration of the map T in (9), which play a role in the study of the global dynamics. In particular we shall analyze the noninvertibility of the map, an important property in the investigation of the topological structures of the attracting sets of the map and their basins of attraction. The second property we present is typical of the maps describing a duopoly model with naive expectations, as the map T is, and it is related to the second iterate of T, i.e., $T \circ T$, which results in a de-coupled map. Such a property, that we shall call *"square separate" property,* allows to deduce the dynamic properties of T by those of a one-dimensional map, as proved in [7]. Finally some analytical results about the fixed points are given, even if they can not be obtained in closed form.

3.1 Noninvertibility

We recall that a map T is noninvertible if given point $p^{'} \in \mathbb{R}^2$ the point $p \in \mathbb{R}^2$ such that $p^{'} = T\,(p)$, i.e., the *rank-1 preimage* of $p^{'}$, may not exist or may be not unique. In other words, a noninvertible map is a correspondence many-to-one, that is, distinct points of the plane may have the same image and points x exist that have no preimage or several rank-1 preimages. Geometrically the action of a noninvertible map can be expressed by saying that it "fold and pleats" the plane, so that distinct points are mapped into the same point. This is the same as saying that several inverses are defined in some point $x \in \mathbb{R}^2$, and these inverses "unfold" the plane.

Considering the map T in (9), the rank-1 preimages of a given point $(u, v) \in \mathbb{R}^2$ are the solutions the algebraic system

$$\begin{cases} u = (\alpha y - \alpha + 1)^2 \\ v = (\beta x - 1)^2 \end{cases}$$

in the unknown variables x and y. It is simple to obtain that four solutions exist iff $u \geq 0$ and $v \geq 0$, given by

$$\begin{array}{lll} T_1^{-1} & : & \left\{ \begin{array}{c} x = \frac{1+\sqrt{v}}{\beta} \\ y = \frac{\alpha-1+\sqrt{u}}{\alpha} \end{array} \right. , \qquad T_2^{-1} : \left\{ \begin{array}{c} x = \frac{1-\sqrt{v}}{\beta} \\ y = \frac{\alpha-1-\sqrt{u}}{\alpha} \end{array} \right. , \\ T_3^{-1} & : & \left\{ \begin{array}{c} x = \frac{1-\sqrt{v}}{\beta} \\ y = \frac{\alpha-1+\sqrt{u}}{\alpha} \end{array} \right. , \qquad T_4^{-1} : \left\{ \begin{array}{c} x = \frac{1+\sqrt{v}}{\beta} \\ y = \frac{\alpha-1-\sqrt{u}}{\alpha} \end{array} \right. . \end{array} \tag{11}$$

The noninvertibility of the map T is so stated and the multivalued inverse relation can be represented as

$$T^{-1} = T_1^{-1} \cup T_2^{-1} \cup T_3^{-1} \cup T_4^{-1}.$$

Then, following the terminology introduced in ([20]) and in [14], we can say that the map T in (9) is a $Z_4 - Z_0$ map, which means that in the plane there is a region of points having four distinct rank-1 preimages and another one whose points have no preimage. Such regions, or *zones*, are separated by the *critical line* LC (see [14],[20]), i.e. the locus of points having two merging rank-1 preimages.

From (9), it is easy to obtain that the critical line is given by two distinct branches, that is $LC = LC^a \cup LC^b$ with

$$\begin{array}{rcl} LC^a & = & \{(x,y) : x = 0\} \\ LC^b & = & \{(x,y) : y = 0\} \end{array} \tag{12}$$

The locus of the merging preimages of the points belonging to the set LC, is the rank-0 critical line LC_{-1}, still made up by two branches

$$LC_{-1} = LC_{-1}^a \cup LC_{-1}^b = \left\{ (x,y) : y = 1 - \frac{1}{\alpha} \right\} \cup \left\{ (x,y) : x = \frac{1}{\beta} \right\} \tag{13}$$

Observe that each branch of LC_{-1} passes through a minimum points of the reaction functions.

In alternative, the critical lines can be also obtained from the Jacobian matrix of the map T, LC_{-1} being the locus of point at which the determinant of the Jacobian matrix vanishes, and $LC = T\left(LC_{-1}\right)$.

Let us verify this assertion. We have

$$LC_{-1} \subseteq J_0 = \left\{ (x,y) \in \mathbb{R}^2 : \det JT\,(x,y) = 0 \right\}$$

where

$$JT\,(x,y) = \left[\begin{array}{cc} 0 & 2\alpha\,(\alpha y - \alpha + 1) \\ 2\beta\,(\beta x - 1) & 0 \end{array} \right].$$

Hence

$$\begin{array}{rcl} \det JT\,(x,y) & = & -4\alpha\beta\,(\beta x - 1)\,(\alpha y - \alpha + 1) = 0 \\ LC_{-1}^a & : & y = 1 - \frac{1}{\alpha};\ \ LC_{-1}^a\text{:}\ \ x = \frac{1}{\beta} \end{array}$$

and

$$\begin{aligned} LC^a &= T\left(LC^a_{-1}\right) = T\left(x, 1-\frac{1}{\alpha}\right) = \{(x,y) : x = 0\} \\ LC^b &= T\left(LC^b_{-1}\right) = T\left(\frac{1}{\beta}, y\right) = \{(x,y) : y = 0\} \end{aligned}$$

that is, exactly the critical lines LC_{-1} and LC in (13) and (12), respectively.

Making use of the critical lines, represented in Fig.1a, we may understand the *Riemann foliation* of the plane $\mathbb{R}^2$ associated with the map T, i.e. the number of superimposed "sheets" which cover the plane giving reason to the number of preimages existing in its different regions. The action of the map T is to fold twice the plane along the coordinate axis (the critical line LC), so that the positive quadrant of the plane, $\mathbb{R}^2_+$, can be considered as made up of 4 sheets, each one associated with a different inverse; on the other side the multivalued inverse relation T^{-1} in (11) unfolds $\mathbb{R}^2_+$ along the critical line of rank-0 LC_{-1}, so that each point of $\mathbb{R}^2_+$ has four distinct preimages located at opposite side with respect to LC_{-1}.

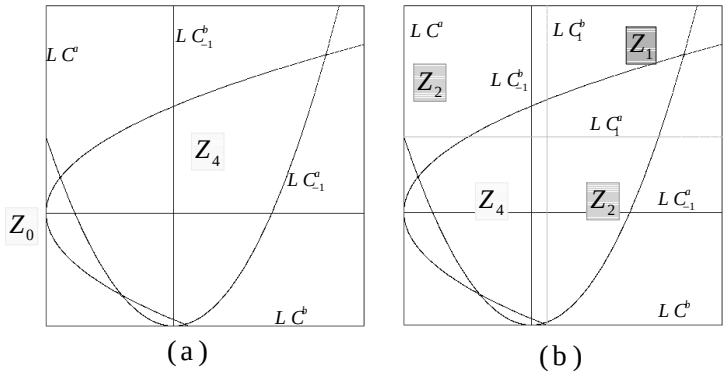

Figure 1: (a). *Riemann foliation of the plane* $\mathbb{R}^2$ *associated with the map* T. (b). *Riemann foliation of the half-plane* $\mathbb{R}^2_+$ *associated with the restriction of the map* T *to the positive half-plane.*

Looking at the inverse relation T^{-1} we can also deduce that $\mathbb{R}^2_+$, the positive quadrant of the plane, is an invariant set for the map T, that is $T\left(\mathbb{R}^2_+\right) = \mathbb{R}^2_+$. Indeed any point of $\mathbb{R}^2_+$ has at least a rank-1 preimage, T_1^{-1}, belonging to the positive quadrant of the plane. Then the model we are considering is well-posed from an economic point of view, since only positive quantities x and y are meaningful. In the following we shall consider the restriction of map T to the positive quadrant of the plane. So doing, we have to define the Riemann foliation of $\mathbb{R}^2_+$, taking into account the coordinates axes, lower boundary of $\mathbb{R}^2_+$, and their images, as observed in [6]. Indeed, given a point $(u,v) \in \mathbb{R}^2_+$, some of its rank-1 preimages may be unfeasible (i.e., may have at least one negative

coordinate) and, looking at T^{-1} in (9), it is simple to obtain that this occurs if $u > (\alpha - 1)^2$ and/or $v > 1$. Then the two half-lines

$$\begin{aligned} LC_1^a &= \{(x, y) : x \geq 0, y = 1\} \\ LC_1^b &= \left\{(x, y) : x = (\alpha - 1)^2, y \geq 0\right\} \end{aligned} \tag{14}$$

separate region of points having a different number of preimages and T (restricted to $\mathbb{R}^2_+$) is a $Z_4 - Z_2 - Z_1$, as illustrated in Fig.1b. Note that LC_1^a and LC_1^b are not critical lines in the sense of [14] and [20], because their points do not have merging preimages. However the essential features of the critical curves theory apply also to such lines because the crossing through them still causes the appearance or disappearance of rank-1 preimages. In (14), we use the symbols LC_1^a and LC_1^b since the half-line are exactly the images of the two branches of the critical line, as it is simple to verify.

3.2 "Square separate" property

As any map describing a Cournot game in which the firms have "naive expectations", the map T has the "*square separate*" property, that is the map T^2 (the second iterate of T) is a de-coupled map, i.e.,

$$T^2(x, y) = T(r_1(y), r_2(x)) = (r_1(r_2(x)), r_2(r_1(y))) = (F(x), G(y)) \tag{15}$$

The maps having this property have been studied in-depth in [7]: In order to keep the paper self-contained we repeat here the main results given in such paper. Further references on this kind of maps are [12], [17] and [4].

The main result is that the dynamic behavior of the map T can be deduced from the one-dimensional map $F(x)$ (or $G(y)$) obtained by the composition of the two reaction functions.

Indeed, there exists a correspondence between the cycles of map $F(x)$ and the cycles of T. In particular, if x^* is a fixed point of F, then $(x^*, r_2(x^*))$ is fixed point of T with eigenvalue $\lambda_1 = F'(x^*)$ and $\lambda_2 = -F'(x^*)$. If x_1^* and x_2^* are fixed points of $F(x)$ then $\{(x_1^*, r_2(x_2^*)), (x_2^*, r_2(x_1^*))\}$ is cycle of period 2 of T, with eigenvalue $\lambda_1 = F'(x_1^*)$ and $\lambda_2 = -F'(x_2^*)$. We deduce that the map T has no saddle fixed points, but saddle cycles may emerge, for example when F has two fixed points, one attracting and one repelling, a saddle cycle of period 2 exists.

Moreover, the number of the cycles of T is not in a one-to-one correspondence with those of F, but increases very quickly: In any case it is always possible to obtain the cycles of T starting from the cycles of F and a general rule to do that is given in [7]. Given the large number of its cycles, it is also immediate to realize that the *multistability*, i.e. the coexistence of several distinct attractors, is a possible outcome of T: In particular, in [7] it is proved that if F has a stable cycle of period $n > 2$ then several stable cycles of T also exist.

The local bifurcations of the one-dimensional map F correspond to bifurcations of T; in fact whenever a bifurcation occurs that causes the appearance

(disappearance) of cycles of the map T, many cycles of the map T simultaneously appear (disappear) at the same parameter values. Such bifurcations of the two-dimensional map are often of particular type (as analyzed in [17]), due to the presence of the two eigenvalues that simultaneously cross the unit circle. A supercritical flip bifurcation of a fixed point of F, gives rise to two cycles of period 4 of T, a stable one and a saddle; a fold bifurcation causes the appearance of two fixed points, one stable and one unstable, as well as a saddle cycle of period 2.

Moreover, when $r_1(y)$ and $r_2(x)$ are noninvertible functions, as in the case we are considering, the function F is a noninvertible map as well, and the attractors of F may also be k-pieces chaotic intervals or Cantor sets. Therefore, the attracting sets of T may have as well a complex structure: Cycles of period k, k-pieces chaotic rectangles or k-cycles chaotic segments.

As we have seen, the coexistence of several attractors is a peculiarity of the Cournot map, then the study of the structure of the corresponding basins of attraction becomes of particular interest in order to anticipate the asymptotic behavior of the Cournot tâtonnement starting from a given initial condition. At this aim we recall that a vertical (horizontal) segment is mapped into a horizontal (vertical) segment by a square separate map and the same holds for preimages: An example has be given in the previous subsection, where the images (LC_1) and the preimages (LC_{-1}) of the critical line LC have been obtained (see Fig.1). Consequently, all the absorbing and the chaotic areas of a Cournot map are rectangles, being bounded by segments of critical lines parallel to the coordinate axes. Moreover, as saddle cycles always have eigenvectors parallel to the coordinates axis (see [7]), their unstable and stable sets are made up by the union of vertical and horizontal segments. Then the basins of attraction of the different attracting sets are rectangles, if connected, or have many components with rectangular shape.

It is worth here to outline two facts: First, the boundaries of absorbing and chaotic areas of T are given by the forward iterates of the critical line, and the branches of the critical line are vertical or horizontal segments passing through the critical values of F; second, the basins boundaries can be built starting from the repelling cycles of F. Indeed, since in noninvertible maps many global bifurcations (also called *contact bifurcations*) result in a contact between a basin boundary and a critical curve segment obtained by the iteration of LC, we obtain that the global bifurcations of the map F correspond to global bifurcations of map T.

In order to summarize, we can say that all the attractors of two-dimensional map T, and their local and global bifurcations, can be obtained from the knowledge of the dynamics of the one-dimensional map F (or G). For that reason in the next sections we shall consider the local and global bifurcations of the map F defined in (15), from which we shall deduce the dynamical behavior of model (9).

3.3 Fixed points

From (15) and (9), we obtain that the one-dimensional map F is given by

$$F(x) = r_1(r_2(x)) = \left(\alpha(\beta x - 1)^2 - \alpha + 1\right)^2 \tag{16}$$

where $(\alpha, \beta) \in \Omega$ given in (10).

F is a fourth degree polynomial, assuming positive values. Its critical points are two local minimum points $c^m_{-1,1} = \frac{1}{\beta}\left(1 - \sqrt{1 - \frac{1}{\alpha}}\right)$, $c^m_{-1,2} = \frac{1}{\beta}\left(1 + \sqrt{1 + \frac{1}{\alpha}}\right)$, with common critical value (in the Julia-Fatou sense) $c^m = 0$ and a local maximum point $c^M_{-1} = \frac{1}{\beta}$ with critical value $c^M = (1 - \alpha)^2$. The W-shaped graph of F in (16) is given in Fig.2, where it is also pointed out that $c^m_1 = F(c^m) = 1$. As already observed for the map T, the critical values c^M and c^m_1 separate the positive half-line $\mathbb{R}_+$ in three intervals characterized by a different number of preimages: In particular we may obtain a $Z_1 - Z_2 - Z_4$ map, as in Fig.2a where $c^M < c^m_1$, or a $Z_1 - Z_3 - Z_4$ map in the opposite case (see Fig.2b).

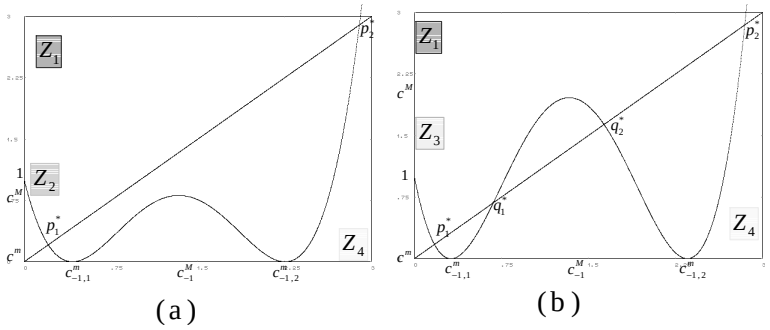

Figure 2: *Graph of the one-dimensional map* $F(x) = r_1(r_2(x))$. (a) *in the case* $c^M < c^m_1 = 1$. (b) *in the case* $c^M > c^m_1 = 1$.

Since it is given by the composition of two functions with negative *Schwarzian derivative* (the two quadratic reaction functions), F has negative Schwarzian derivative. Hence the map F can have at most two coexisting attractors, each with one critical value in its basin of attraction (see [25]).

Being $F(x) = x$ a fourth degree polynomial equation, the map F can have at most four fixed points. Two fixed points certainly exist: $p^*_1 \in \left(0, c^m_{-1,1}\right)$, since in such an interval F decreases from 0 to 1 and $c^m_{-1,1} < 1$, and $p^*_2 \in \left(c^m_{-1,2}, +\infty\right)$. The existence of this latter follows by the observation that, $F\left(c^m_{-1,2}\right) = 0 < c^m_{-1,2}$ and, being $\lim_{x\to+\infty} \frac{F(x)}{x} = +\infty$, we obtain that there exist a $x_1 > 0$ such that $F(x) > x$ for any $x > x_1$. Moreover, since the map F is definitively expanding, p^*_2 has to separate unbounded and bounded (if existing) trajectories. We can so state the following

Proposition 1 *Two fixed points of F always exist. The largest one, p_2^*, is unstable for any $(\alpha, \beta) \in \Omega$.*

From Proposition 1, we obtain that the set $\boldsymbol{F}_1 \times \boldsymbol{F}_2$ of bounded trajectories (*feasible trajectories*) of the map T in (9) is included in the set $\boldsymbol{X} \times \boldsymbol{Y}$, where

$$\begin{aligned} \boldsymbol{X} &= \left\{(x,y) \in \mathbb{R}_+^2 : 0 < x < p_2^*\right\} \\ \boldsymbol{Y} &= \left\{(x,y) \in \mathbb{R}_+^2 : 0 < y < r_2\left(p_2^*\right)\right\}. \end{aligned} \tag{17}$$

The topological structure of the strategic sets $\boldsymbol{F}_1, \boldsymbol{F}_2$ of the two firms depend on the parameter value, but, as we shall, generally, we have that $\boldsymbol{X} \equiv \boldsymbol{F}_1$ and $\boldsymbol{Y} \equiv \boldsymbol{F}_2$, as in the example of Fig.3 where the reaction functions and the critical lines are represented as well. The gray area in the Fig.3, denoted by $B(\infty)$, represents the points which give rise to divergent trajectories; its complementary set (light gray area) is the sets of point having bounded trajectories (feasible trajectories), which generally includes one or more attractors at finite distance. At the parameter constellation of Fig.3, the Cournot equilibrium point P_1^* is the unique attractor of the map T and its basin of attraction is given by the light gray points.

In Fig.3, the reaction functions intersect twice, and only two fixed points of T (and of F) exist, but as we said above, the existence of four fixed points is a possible outcome.

Proposition 2 *In the parameter set $\Omega = \{(\alpha, \beta) : \alpha > 1, \beta > 0\}$, a fold bifurcation of the map F occurs at the crossing of the curve*

$$\begin{cases} \alpha = \frac{(3t+4)^2}{8(t+2)} \\ \beta = \frac{2(t+2)}{t^2(3t+4)} \end{cases} \tag{18}$$

where the parameter t is strictly positive.

Proof. The proof follows by the observation that between the two distinct solutions of the system

$$\begin{cases} \left(\alpha\left(\beta x - 1\right)^2 - \alpha + 1\right)^2 = x \\ 4\alpha\beta\left(\beta x - 1\right)\left(\left(\beta x - 1\right)^2 - \alpha + 1\right) = 1 \end{cases}$$

in the variables α and β, (18) is the unique belonging to the parameter set Ω. ■

From Proposition 2 we deduce that, when the curve (18) is crossed, two further fixed points appear, one unstable, q_1^*, and one stable q_2^*, as in Fig.2b, located between p_1^* and p_2^*. The appearance of these points may create a bistability situation for the map F, and consequently a multistability for T. The global analysis of these situations will be the object of the next section.

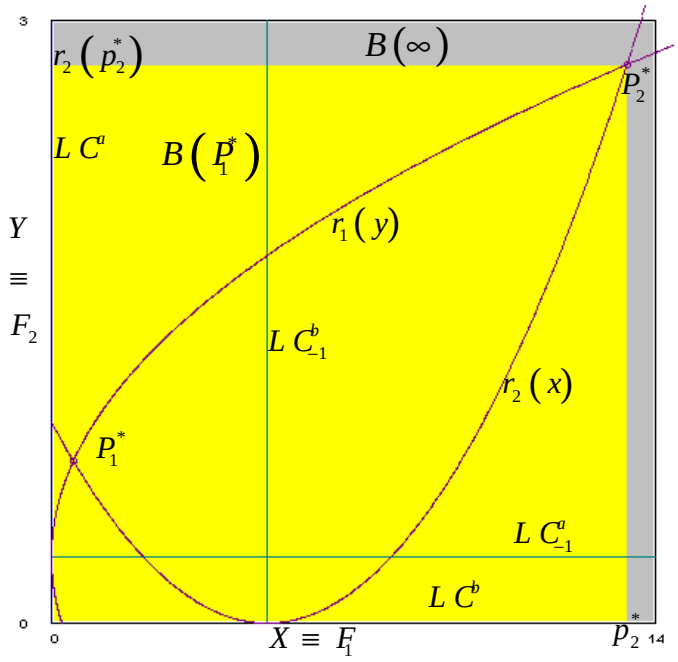

Figure 3: *The phase-space of T at $\alpha = 1.49$ and $\beta = 0.2$. The Cournot equilibrium point P_1^* is the unique attractor and the light gray area denotes its basin of attraction. The gray points give rise to divergent trajectories. The reaction functions and the strategic sets are represented, as well.*

4 Multistability and basins of attraction

As we have seen in the previous Section, multistability is a typical feature of the map T in (9), due to its "square separate" property. Indeed, analyzing the dynamical behaviour of the trajectories of the map F, it is simple to verify that, also in the case in which only two fixed points exist (one stable and one unstable), a flip bifurcation of the stable one occurs, causing the appearance of a stable period 2 cycle. Such a flip bifurcation is the starting point of the usual cascade of period doubling bifurcations towards chaos and then there exist some parameter constellations at which a stable cycle, of period 4 or higher, can be detected for the map F. Consequently, the map T exhibits the coexistence of many cycles. For example, in the simpler case, when the map F has a stable cycle of period 4, two stable cycles of period 8 exist for T. We don't enter into the details of the multistability situations associated with a stable cycles of period larger than 2, of the map F, since many examples can be found in the duopoly model literature (see, among others, [4], [7] and [8]).

In order to investigate some different situations of multistability, let us start from the analysis of the bifurcation diagrams illustrated in Fig.4, in which dif-

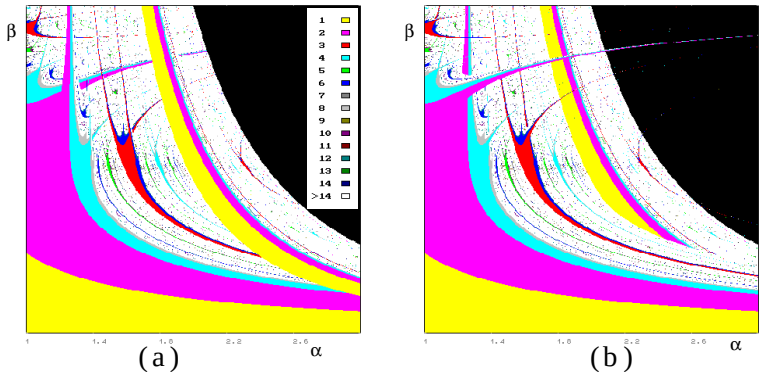

Figure 4: *Bifurcation diagrams of the map F in the (α, β)-parameter plane obtained with* (a) *initial condition c^M.* (b) *initial condition c^m. The different gray tones correspond to different periods of the cycles, in accordance with the legenda. The black area denotes unbounded trajectories.*

ferent colors correspond to stable cycles of different period: Such bifurcation diagram have been obtained considering the long run behavior of the trajectories generated by the iteration of the map F, as the two parameters α and β are varied: In Fig.4a the initial condition is the critical point c^M (local maximum of F) whereas in Fig.4b the local minimum c^m has been considered as starting point of the trajectories. From Fig.4a, it is possible to appreciate the fold bifurcation curve, given by the lower frontier of the smaller area in color 1, as well as the period doubling bifurcation cascade occurring twice, starting either from the fixed points p_1^* and q_2^*. Comparing Fig.4a with Fig.4b, it is also possible to observe that there exist many parameter constellations at which the two critical points have a different limit set, and the major part of them crosses the fold bifurcation curve. Indeed, as a consequence of the fold bifurcation two further fixed points appear, one stable, q_2^*, and one unstable, q_1^*, generally coexisting with the pre-existing attracting set A of the map: The unstable fixed point q_1^* separates the basins of attraction of q_2^* and A. Observe that for map F, it may also happen that no multistability exists after the occurrence of the fold bifurcation: This occurs because the appearance the repelling fixed point q_1^* causes the disappearance of the pre-existing chaotic interval A, since q_1^* belong to the boundary of A.Let us analyze more deeply the multistability situation due to the occurrence of the fold bifurcation in the simplest case: We consider a parameter constellations at which there exist two disjoint attracting sets, each one made up by a fixed point, as in Fig.5.

We obtain such a figure when $\alpha = 4.8$ and $\beta = 0.08$ and at these parameter values two disjoint absorbing intervals exist: $I^m = [c^m, c_1^m]$ and $I^M = \left[c_1^M, c^M\right]$, as shown in Fig.5a. This is a sufficient condition for the existence of two attractors, indeed the fixed point p_1^* is stable and belongs to I^m, whereas the stable

fixed point q_2^*, appeared at the fold bifurcation, belongs to I^M. In Fig.5b the basin of attraction of the two stable fixed points are shown, the light gray and gray points along the diagonal: We can observe that, as explained in Section 3, the bounded trajectories belong to the interval $[0, p_2^*]$ and the two basins are disconnected sets, because the noninvertibility of the map F. Indeed, the fixed point q_1^* has three rank-1 preimages, q_1^* itself and two extra preimages ($q_{1,-1}^a$ and $q_{1,-1}^b$) located at the right side with respect to q_1^* and at opposite side with respect to $c_{-1,2}^m$. Moreover each one of these preimages gives rise to sequence of preimages of increasing rank of p_1^*, accumulating at p_2^*, and this explains the structure of the basins of attraction. The immediate basin[2]of p_1^* is the interval

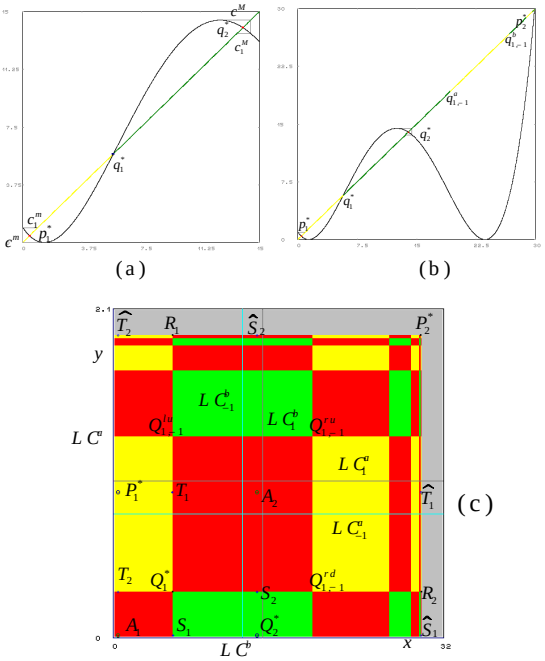

Figure 5: $\alpha = 4.8$ and $\beta = 0.08$. (a). *Two disjoint absorbing interval exist:* $I^m = [c^m, c_1^m]$ *and* $I^M = \left[c_1^M, c^M\right]$. *The stable fixed point* p_1^* *belongs to* I^m *while the stable fixed point* q_2^* *belongs to* I^M. (b). *The basin of attraction of the two stable fixed points are shown along the line* $x = y$ *in light gray and gray. (c). Phase space of the map* T. *Three attractors coexist: the two fixed points,* P_1^* *and* Q_2^*, *and a cycle of period 2 whose periodic points are* A_1, A_2. *Their basins of attraction are represented in different gray tones and have infinitely many rectangular components. The side of the rectangles are made up by the stable sets of the saddle 2-cycle* S *and* T, *the vertices being the preimages of the repelling fixed point* Q_1^*. *Being* $Q_1^* \in Z_4$, *the rank-1 ones are* Q_1^* *itself,* $Q_{1,-1}^{rd}$, $Q_{1,-1}^{ru}$, $Q_{1,-1}^{lu}$ *located at opposite side with respect to the two branches of* LC_{-1}.

$[0, q_1^*)$, whereas that of q_2^* is bounded by q_1^* and $q_{1,-1}^a$, and the other preimages of q_1^* bound the different components of the basin; more precisely we obtain that

$$\begin{aligned} B(q_2^*) &= \left(q_1^*, q_{1,-1}^a\right) \cup \left(q_{1,-1}^b, q_{1,-2}^a\right) \cup \left(q_{1,-2}^b, q_{1,-3}^a\right) \cup ... \\ B(p_1^*) &= [0, q_1^*) \cup \left(q_{1,-1}^a, q_{1,-2}^b\right) \cup \left(q_{1,-2}^a, q_{1,-2}^b\right) \cup ... \end{aligned}$$

Obviously, the bistability situation and the associated complex structure of the basins reflects in the dynamics of the two-dimensional map T, being complicated by the existence of an attracting cycle period 2, as explained in Section 3: The corresponding two-dimensional phase-space is shown in Fig.5c.

The attractors of T are the two fixed points, $P_1^* = (p_1^*, r_2(p_1^*))$ and $Q_2^* = (q_2^*, r_2(q_2^*))$, and a cycle $\mathcal{A}$ of period 2 whose periodic points are $A_1 = (p_1^*, r_2(q_2^*))$ and $A_2 = (q_2^*, r_2(p_1^*))$. The corresponding basins of attraction are still disconnected sets and, as expected, have rectangular components: Their structure may be explained by means of the coexisting unstable cycles and their preimages of any rank. Indeed, as shown in Fig.5c, besides the two repelling fixed points, P_2^* and Q_1^*, there also exist a repelling period 2 cycle $\mathcal{R}$ and 4 saddle cycles always of period 2: S, T, $\widehat{\mathcal{S}}$ and $\widehat{T}$. The repelling cycle $\mathcal{R}$ and the saddle cycles $\widehat{\mathcal{S}}$ and $\widehat{T}$ belong to the frontier of the bounded trajectories, made up by the stable sets of the saddle $\widehat{\mathcal{S}}$ and $\widehat{T}$ and by the repelling cycles P_2^* and $\mathcal{R}$ and all their preimages of any rank.

The stable sets of the two saddle cycles S and T are the separatrices of the three basins of attraction: In particular, the stable set of S separates the basins of Q_2^* and the cycle $\mathcal{A}$, whereas the trajectories converging to P_1^* have the stable set of T as boundary. It is worth to observe that, being the map T noninvertible, the stable set of a saddle is not necessarily a manifold (as in the case of the invertible maps) and in this case is a disconnected set. Moreover, the vertices of the rectangular components of the basins are the preimages of any rank of the repelling fixed point Q_1^*.

We have commented just a particular case, the simplest one, but similar arguments apply to the more complex multistability situations: We always have that the basins of the coexisting attractors of the two-dimensional map T are separated by the stable sets of some saddle cycles and have a rectangular shape with vertices the preimages of the existing repelling cycles.

Let us now return to the bifurcation diagrams of Fig.4, in order to describe a quite different situation.

Indeed, up to now, we have considered multistability situations occurring when the one-dimensional map F has four fixed points, but comparing Fig.4a and Fig.4b it emerges that multistability may even occur when F has only two fixed points (and the two disjoint absorbing intervals do not exist). For example, the portions of the bifurcation diagrams highlighted by a circle are located below the fold bifurcation curve and at the corresponding values of the parameters a stable cycle of period 4 coexists with a stable cycle of period 2. To better

[2] i.e., the largest connected component of the basin containing the fixed point.

investigate the dynamical behavior of F at these parameter constellations we fix the value of α and consider the bifurcation diagrams obtained at increasing value of β from 1.3, shown in Fig.6. Observing such a figure, we deduce that at $\alpha = 1.25$ a bistability exists in a quite narrow range of the parameter β (approximately when $\beta \in [1.426, 1.575]$) and it starts with the coexistence of two cycle of period 2 (not detectable in Fig.4 since the two cycles have the same period and both represented in color 2). The bistability is due to a fold bifurcation (of the map F^2, second iterate of F) occurring at a certain value of β, say β_f, and causing the appearance of two cycles of period 2, one stable, say $\widetilde{\mathcal{C}}$, and one unstable, say $\widetilde{\mathcal{R}}$: After the occurrence of the fold bifurcation, the critical point c^m jumps to the "new" cycle $\widetilde{\mathcal{C}}$, while c^M still converge to the "old" one, say $\mathcal{C}$. As the parameter β is increased, the cycle $\widetilde{\mathcal{C}}$ undergoes a sequence of period doubling bifurcations which ends in a two-pieces chaotic attractor. The bistability persists until the repelling cycle $\widetilde{\mathcal{R}}$, a periodic point of which is qualitatively represented in Fig.6a (dotted curve), has a contact with the chaotic interval: This global bifurcation of F causes the sudden disappearance of the two-pieces chaotic attractor, restoring the convergence of the trajectory starting from c^m to the cycle $\mathcal{C}$.

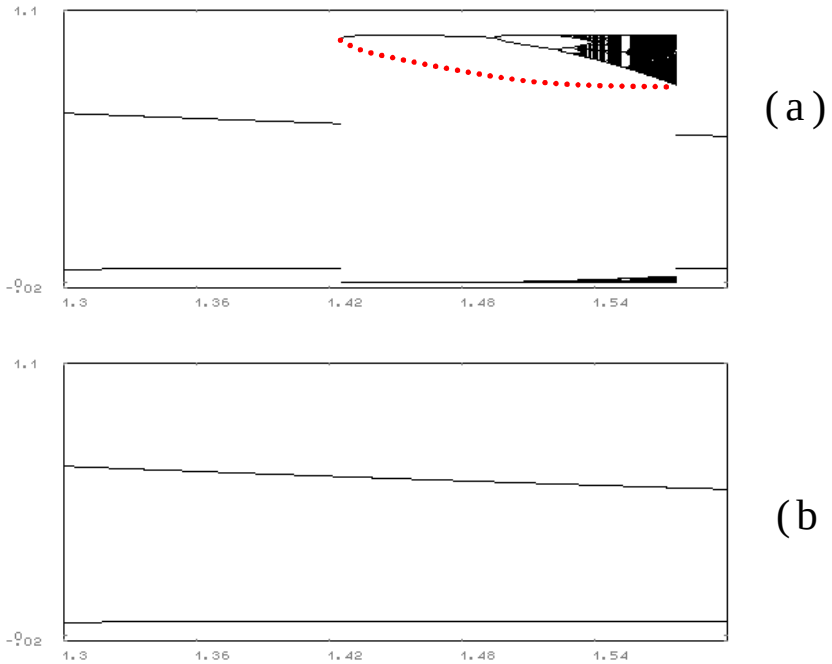

Figure 6: *Bifurcation diagrams of the map F at $\alpha = 1.25$, when β increases.* (a). *The initial condition is the critical value c^m (minimum value of F).* (b) *The initial condition is the critical value c^M (maximum value of F).*

The corresponding dynamics of the map F and T are represented in Fig.7ab and Fig.7cd, respectively. In particular, Fig.7a is obtained after the fold bifurcation of F^2: The two coexisting cycles are represented together with their basins of attraction (light gray and gray points along the diagonal). The basins of attraction are disconnected sets and separated by the repelling cycle $\widetilde{\mathcal{R}}$ and its preimages of any rank, as the graph of the second iterate of F allows to appreciate. Observe that the two basins have infinitely many components and the smaller ones are located around the repelling fixed points p_1^*, and its preimages of any rank.

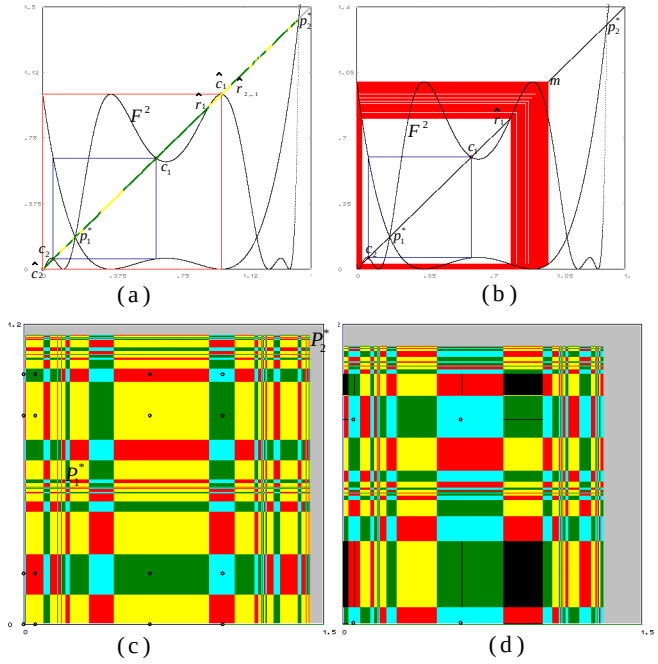

Figure 7: (a) $\alpha = 1.25$ *and* $\beta = 1.45$. *The basins of attraction of the two cycles of period 2, separated by the preimages of any rank of* p_1^* (b) $\alpha = 1.25$ *and* $\beta = 1.575$. *Close to the homoclinic bifurcation of the repelling 2 cycle* $\widehat{\mathcal{R}}$. *(c)* $\alpha = 1.25$ *and* $\beta = 1.45$. *Phase-space of* T*: Four coexisting attracting cycles of period 4 exist. Their basins have the characteristic rectangular structure. (d)* $\alpha = 1.25$ *and* $\beta = 1.575$. *The map* T *exhibits the multistability between a cycle of period 4, two 4-pieces chaotic attractors and 4-pieces chaotic intervals.*

This situation reflects in the dynamical behavior of the two-dimensional map, as shown in Fig.7c. The map T exhibits four coexisting attracting cycle whose basins have the usual rectangular structure. The rectangular components of the basins are separated by the stable set of the several saddle cycles existing, as in the case commented above. It is worth to observe that the existence of infinitely

many preimages of the repelling cycles, makes uncertain the long run behavior of the trajectories starting close to P_1^*, where narrow components of any basin exist.

When β increases from the bifurcation value β_f, the cycle $\widetilde{\mathcal{C}}$ undergoes a first flip bifurcation which gives rise to a stable cycle of period 8 and makes $\widetilde{\mathcal{C}}$ unstable; at its turn the period 8 cycle becomes unstable and an attracting cycle of period 16 appears, and so on until all the cycle of even period are created at β_o^*. The parameter value β_o^* is a limit point of a decreasing sequence of homoclinic bifurcation values for the map F^2, each one of them causing the appearance of cyclical chaotic intervals, made up by a different even number of pieces. The last one of these homoclinic bifurcations, occurring at the largest value of β, regards the cycle $\widetilde{\mathcal{R}}$, born via fold bifurcation together with $\widetilde{\mathcal{C}}$. In Fig.7b, the bifurcation has not yet occurred but α and β are very close to the bifurcation values: Looking at the map F^2, we can observe that the point m, critical value of F^2, is mapped in a point very close to a periodic point, $\widehat{r}_1$, of $\widetilde{\mathcal{R}}$. At the bifurcation the point $\widehat{r}_1$ merges with $F^2(m)$, so that the two-pieces chaotic interval takes up the whole of its immediate basin (and in the range $[\widehat{r}_1, m]$, F^2 behaves like the logistic map $f(x) = 4x(1-x)$). Immediately after the homoclinic bifurcation, the chaotic attractor sudden disappears and the bistability window is closed, the "old" cycle $\mathcal{C}$ remaining the unique attractor of the map F.

At the same parameter values of Fig.7b, the two-dimensional map T exhibits a multistability situation between a cycle of period 4, two 4-pieces chaotic attractor with rectangular components and two 4-pieces chaotic intervals, as shown in Fig.7d. We understand that a global bifurcation is coming since the boundaries of the chaotic areas (or intervals) and of their basins of attraction are very close each other. At the bifurcation, they simultaneously have a contact and immediately after the chaotic attractors sudden disappear, leaving the cycle of period 2 as unique attractor of the map T.

Before to conclude this Section, let us give some further insights about the structure of the strategic sets, $\boldsymbol{F}_1$ and $\boldsymbol{F}_2$, of the firms, i.e., the sets from which the production choices x and y are taken in order to obtain feasible (bounded) trajectories. In the previous Section, we have seen that $\boldsymbol{F}_1 \times \boldsymbol{F}_2$ is a subset of the $\boldsymbol{X} \times \boldsymbol{Y}$, where the sets $\boldsymbol{X}$ and $\boldsymbol{Y}$ are defined in (17). It is simple to realize that when the repelling fixed point p_2^* of the one-dimensional map F (or, alternatively, P_2^* of the two-dimensional map T) has a unique rank-1 preimage, p_2^* (P_2^*) itself, the strategic sets $\boldsymbol{F}_1$ and $\boldsymbol{F}_2$ are intervals coinciding with $\boldsymbol{X}$ and $\boldsymbol{Y}$, respectively. This is exactly the case of the examples given above, where the set of bounded trajectories was the connected set $\boldsymbol{X} \times \boldsymbol{Y}$. But when some further rank-1 preimages of p_2^* (or P_2^*) emerge, $\boldsymbol{F}_1$ and $\boldsymbol{F}_2$ undergo a global bifurcation which causes a qualitative change in their topological structure and become proper subsets of $\boldsymbol{X}$ and $\boldsymbol{Y}$, respectively. Once more this bifurcation is a *contact* one, since it occur when p_2^* merge with the critical value (maximum of F) $c^M = (\alpha - 1)^2$ or with the first iterate of the critical value c^m, i.e., with $c_1^m = 1$. Moreover, in both cases, given the Riemann foliation of the map F

shown in Fig.2a, at the bifurcation at least a sequence of preimages of increasing rank, converging to p_2^*, appear: This means that a *snap-back repeller bifurcation* occurs (see [20], [19]), after which infinitely many homoclinic orbits of p_2^* appear and chaotic dynamics exist in the set $[0, p_2^*]$. As a consequence, the set $\boldsymbol{X}$, and $\boldsymbol{Y}$ as well, has a *fractal* structure since it contains a Cantor set made up by infinitely many repelling cycles plus the limit points of such cycles when the period tends toward infinity plus the arborescent sequences of preimages of all these points.

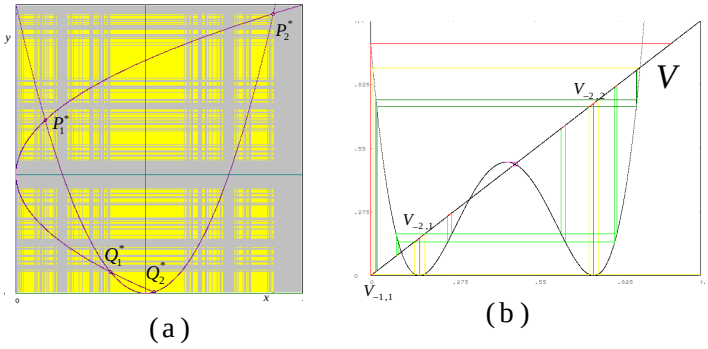

Figure 8: $\alpha = 1.7$ *and* $\beta = 2.21$.(a) *The disconnected basin of attraction of the fixed point* Q_2^* *with its fractal boundary due to the snap-back repeller bifurcation of the expanding fixed point* P_2^*. (b). *The interval* V *is represented together with some of its preimages. Each one of the rank-2 preimages of* V, $V_{-2,1}$ *and* $V_{-2,2}$, *gives rise to an arborescent sequences of preimages, whose construction is suggested.*

An example is shown in Fig.8, where the snap-back repeller bifurcation is due to the merging of p_2^* and $c_1^m = 1$, occurring when $\beta = 2$. As β increases from the value 2, the set of the bounded trajectories of the map T sudden has a complex topological structure, as illustrated in Fig.8a where the set $\boldsymbol{F}_1 \times \boldsymbol{F}_2$ is the basin of attraction of the stable node Q_2^*. The mechanism which gives rise to this complex structure is explained in Fig.8b, making use of the one-dimensional map F. We start from the interval V, whose extrema are 1 and the rank-1 preimage of p_2^* different from the fixed point itself. The preimages of any rank of this set V correspond to the "holes" existing in the set $\boldsymbol{X}$, since the points in them have unbounded trajectories. We may observe that V has a rank-1 preimage located in a right neighborhood of the critical value $c^m = 0$. Then two pairs of preimages of rank-2 exist, each one located at opposite side with respect to a minimum value and merging in it, i.e., the sets $V_{-2,1}$ and $V_{-2,2}$ in Fig.8b. Both these sets give rise to an arborescent sequence of preimages which explain the complex structure of the set $\boldsymbol{F}_1$ and of its companion set $\boldsymbol{F}_2$.

5 Conclusion

In this paper a Cournot duopoly model with complementary goods, recently proposed by Matsumoto and Nonaka in [18], is considered. The map T describing the model is a two-dimensional noninvertible one and, as usually it occurs in Cournot maps associated with the naive expectations assumption, has the "square separate" property, that is the second iterate of T is such that $T^2(x,y) = (F(x), G(y))$. This implies that the asymptotic behavior of T can be obtained by the analysis of the dynamical properties of the one-dimensional map F (or G). A large economic literature exists on such kind of maps (see, among others, [24], [12], [22], [17], [6], [8], [23] and references therein) from which it emerge that the family of maps at which T belongs typically gives rise to the coexistence of several attractors. Just the multistability, and the global dynamics associated with, was our concern in the study of the model, so that no overlapping exists with [18], where the emphasis was on chaotic dynamics.

We have seen that many multistability situations may be detected and associated with different reasons.

A first cause of multistability is the existence of stable cycle of period $n > 2$ of the one-dimensional map F: This case has not been dealt in the present paper, since many analogous situations have been discussed in the papers cited above.

We have dealt with the multistability situations associated with the particular shape of F, which is a bimodal map having negative Schwarzian derivative. The first situation we have considered is associated with the existence of four fixed points of the map F, two of them appearing via fold bifurcation at a certain bifurcation value. The second one, has been detected when only two fixed points exist for F, due to a fold bifurcation of the second iterate of F. In both cases the structure of the basins of attraction of the coexisting attractors of the map T as been analyzed, as well as their qualitative changes, due to global bifurcations.

Finally some results are been obtained about the strategic sets of the firms, i.e. the sets at which their production decisions must belong: We have seen that the transition from connected sets into fractal sets may occur through a snap-back repeller bifurcation of a expanding fixed point of F.

References

[1] R. Abraham, L. Gardini, C. Mira, 1997. *Chaos in discrete dynamical systems (a visual introduction in two dimensions)*, Springer-Verlag:New York.

[2] A. Agliari, 2001. Global bifurcations in the basins of attraction in noninvertible maps and economic applications, *Nonlinear Analysis, T.M.&A.* 47/8, pp. 5241-5252.

[3] A. Agliari, L. Gardini, D. Delli Gatti, M. Gallegati, 2000. Global dynamics in a nonlinear model of the equity ratio, *Chaos, Solitons & Fractals* 11, pp. 961-985

[4] A. Agliari, G. I. Bischi, L. Gardini, 2002. Some methods for the global analysis of dynamic in games represented by iterated noninvertible maps, In: *Oligopoly Dynamics Models and Tools,* (T. Puu and I. Sushko Ed.s), Springer-Verlag:New York, pp. 31-83.

[5] A. Agliari and T. Puu 2002. A Cournot duopoly model with bounded inverse demand, In: *Oligopoly and Complex Dynamics: Tools and Models*, (T. Puu and I. Sushko Ed.s), Springer-Verlag:New York, pp. 171-194.

[6] A. Agliari, L. Gardini, T. Puu, 2005. Global bifurcations in duopoly when the Cournot point is destabilized via a subcritical Neimark bifurcation, *International Game Theory Review* 7, in press.

[7] G.I. Bischi, C. Mammana, L. Gardini, 2000. Multistability and cyclic attractors in duopoly games, *Chaos, Solitons and Fractals* 11, pp. 543-564.

[8] G.I. Bischi, M. Kopel, 2001. Equilibrium Selection in a Nonlinear Duopoly Game with Adaptive Expectations, *Journal of Economic Behavior and Organization* 46, pp. 73-100.

[9] G.I. Bischi, M. Kopel, 2003. Multistability and path dependence in a dynamic brand competition model, *Chaos, Solitons and Fractals* 18, pp. 561-576.

[10] W.A. Brock, C.H. Hommes, 1997. A Rational Route to Randomness. *Econometrica* 65, pp. 1059-1095.

[11] A. Cournot, 1938. *Récherches sur les principes matématiques de la théorie de la richesse*, Hachette:Paris.

[12] R.D. Dana, L. Montrucchio, 1986. Dynamic complexity in duopoly games, *Journal of Economic Theory* 40, pp. 40-56.

[13] Dieci, R., Bischi, G.I., Gardini, L., 2001. Multistability and role of noninvertibility in a discrete-time business cycle model. *Central European Journal of Operation Research* 9, pp. 71-96.

[14] I. Gumoski, C. Mira, 1980. *Dynamique chaotique*, Cepadeus Editions:Toulose.

[15] M. Kopel, 1997. Improving the performance of an economic system: controlling chaos, *Journal of Evolutionary Economics* 7, pp. 269-289.

[16] Lorenz, H.W., 1992. *Multiple attractors, Complex Basin Boundaries, and Transient Motion in Deterministic Economic Systems.* In G. Feichtinger (Ed.), Dynamic Economic Models and Optimal Control. Amsterdam:North-Holland, pp. 411-430.

[17] R. Lupini, S. Lenci, L. Gardini, 1997. Bifurcations and multistability in a class of two dimensional endomorphism, *Nonlinear Analysis T. M. & A.* 28, pp. 61-85.

[18] A. Matsumoto, Y. Nonaka, 2005. Statistical dynamic in chaotic Cournot model with complementary goods, *Journal of Economic Behavior and Organization,* forthcoming.

[19] Marotto F.R., 1978. Snap-back repellers imply chaos in $\mathbb{R}^n$, *J. Math. Anal. Appl.* 63, pp. 199-223.

[20] C. Mira, L. Gardini, A. Barugola, J.C. Cathala, 1996. *Chaotic dynamics in two-dimensional noninvertible maps*, World Scientific:Singapore.

[21] T. Poston and I. Stewart, 1978. *Catastrophe Theory and its Applications.* Pitman Ltd.:London.

[22] T. Puu, 1991. Chaos in duopoly pricing, *Chaos, Solitons & Fractals* 1, pp. 573-581.

[23] Puu, T., Sushko, I., (Eds), 2002. *Oligopoly Dynamics: Models and Tools.* Springer Verlag:New York.

[24] D. Rand, 1978. Exotic phenomena in games and duopoly models. *J. Math. Econ.* 5, pp. 173-184.

[25] D. Singer, 1978. Stable orbits and bifurcation of maps of the interval, *SIAM J. App. Math.* 35, pp. 260-267.